Targeted disruption of the mouse colony-stimulating factor 1 receptor gene results in osteopetrosis, mononuclear phagocyte deficiency, increased primitive progenitor cell frequencies, and reproductive defects

Xu-Ming Dai, Gregory R. Ryan, Andrew J. Hapel, Melissa G. Dominguez, Robert G. Russell, Sara Kapp, Vonetta Sylvestre, and E. Richard Stanley

The effects of colony-stimulating factor 1 (CSF-1), the primary regulator of mononuclear phagocyte production, are thought to be mediated by the CSF-1 receptor (CSF-1R), encoded by the c-*fms* proto-oncogene. To investigate the in vivo specificity of CSF-1 for the CSF-1R, the mouse *Csf1r* gene was inactivated. The phenotype of *Csf1*$^{-}$/*Csf1r*$^{-}$ mice closely resembled the phenotype of CSF-1-nullizygous *(Csf1*^{op}/*Csf1*^{op}*)* mice, including the osteopetrotic, hematopoietic, tissue macrophage, and reproductive phenotypes. Compared with their wild-type littermates, splenic erythroid burst-forming unit and high-proliferative potential colony-forming cell levels in both *Csf1*^{op}/*Csf1*^{op} and *Csf1*$^{-}$/*Csf1r*$^{-}$ mice were significantly elevated, consistent with a negative regulatory role of CSF-1 in erythropoiesis and the maintenance of primitive hematopoietic progenitor cells. The circulating CSF-1 concentration in *Csf1r*$^{-}$/*Csf1r*$^{-}$ mice was elevated 20-fold, in agreement with the previously reported clearance of circulating CSF-1 by CSF-1R–mediated endocytosis and intracellular destruction. Despite their overall similarity, several phenotypic characteristics of the *Csf1r*$^{-}$/*Csf1r*$^{-}$ mice were more severe than those of the *Csf1*^{op}/*Csf1*^{op} mice. The results indicate that all of the effects of CSF-1 are mediated via the CSF-1R, but that subtle effects of the CSF-1R could result from its CSF-1–independent activation. (Blood. 2002;99:111-120)

Introduction

Colony-stimulating factor 1 (CSF-1) regulates the survival, proliferation, and differentiation of mononuclear phagocytic cells and is the primary regulator of mononuclear phagocyte production in vivo.[1,2] However, CSF-1 also regulates cells of the female reproductive tract and plays an important role in fertility.[3,4] The effects of CSF-1 are mediated by a high-affinity receptor tyrosine kinase (CSF-1R)[5-8] encoded by the c-*fms* proto-oncogene.[9] The CSF-1R is expressed on primitive multipotent hematopoietic cells,[10,11] mononuclear phagocyte progenitor cells,[12] monoblasts, promonocytes, monocytes,[5,6] tissue macrophages,[6,13-15] osteoclasts,[16] B cells,[17,18] smooth muscle cells,[19] and neurons.[20,21] CSF-1R messenger RNA (mRNA) is expressed in Langerhans cells,[22] in the female reproductive tract, in oocytes and embryonic cells of the inner cell mass and trophectoderm,[23] in decidual cells,[24-26] and in cells of the trophoblast.[24,25] The expression of the CSF-1R on primitive hematopoietic cells that are unable to proliferate in vitro in response to CSF-1 alone[10,11] but are able to proliferate and differentiate if stimulated with combinations of CSF-1 and other hematopoietic growth factors[10,11,27] suggests that CSF-1R is involved in the regulation of more primitive hematopoietic cells than those that form macrophage colonies in vitro in response to CSF-1 alone.

Mice homozygous for the mutation *osteopetrotic*[28] possess an inactivating mutation in the coding region of the CSF-1 gene and are devoid of detectable CSF-1.[29,30] These *Csf1*^{op}/*Csf1*^{op} mice are osteopetrotic because of an early and marked deficiency of osteoclasts[28] that spontaneously recovers with age,[31,32] probably because of the action of vascular endothelial growth factor.[33] However, the phenotype of these mice is pleiotropic.[3] They are toothless; have low body weight, low growth rate, and skeletal abnormalities; and are deficient in tissue macrophages.[2,28,30,34,35] They have defects in both male and female fertility, neural development, the dermis, and synovial membranes.[3] The pleiotropic phenotype of the *Csf1*^{op}/*Csf1*^{op} mouse may be due to a reduction in trophic and/or scavenger functions of the tissue macrophages regulated by CSF-1, secondary to the reduction of their concentration in tissues,[2] because outside the female reproductive tract the CSF-1R is primarily expressed in mononuclear phagocytes.[1,3] However, it is possible that some of these effects may also be due to loss of function of other cells such as neuronal cells and muscle precursors, which have also been reported to express the CSF-1R.[20,36]

To address the questions of whether CSF-1 activates other receptors besides the CSF-1R and, conversely, whether the CSF-1R mediates the response to ligands other than CSF-1, we have carried out the targeted inactivation of the CSF-1R gene. The present study describes the phenotype of mice homozygous for a targeted CSF-1R–null mutation and compares it with the phenotype of *Csf1*^{op}/*Csf1*^{op} mice. The slightly more severe phenotype of *Csf1r*$^{-}$/*Csf1r*$^{-}$ over *Csf1*^{op}/*Csf1*^{op} mice indicates that the effects of CSF-1

From the Department of Developmental and Molecular Biology, Albert Einstein College of Medicine, Bronx, NY.

Submitted May 23, 2001; accepted August 31, 2001.

Supported by grant CA32551 from the National Institutes of Health (E.R.S.); grant 5P30-CA13330 from the Albert Einstein College of Medicine Cancer Center; an American Cancer Society Fellowship (A.J.H.); a Yamagiwa-Yoshida Memorial UICC International Cancer Study Grant (A.J.H.); and an American Society of Hematology fellowship (G.R.R.).

Reprints: E. Richard Stanley, Dept of Developmental and Molecular Biology, Albert Einstein College of Medicine, 1300 Morris Park Ave, Bronx, NY 10461; e-mail: rstanley@aecom.yu.edu.

The publication costs of this article were defrayed in part by page charge payment. Therefore, and solely to indicate this fact, this article is hereby marked "advertisement" in accordance with 18 U.S.C. section 1734.

are uniquely mediated through the CSF-1R and that subtle effects of the CSF-1R could result from its CSF-1–independent activation.

Materials and methods

Construction of the *Csf1r* gene-targeting vector

Mouse *Csf1r* 5′ promoter region and exon 2 region primers included cfms-75F, 5′-GGC ACG GGG CTC CCA GCT GCT AGT TCT GTG-3′, and cfms-497R, 5′-AAG GGC AGA TGA GAA AGG TAT GAA GAA TGT-3′; and mouse *Csf1r* 3′ terminal region and exon 22 sequence primers included cfms-3024F, 5′-CCT CAG CTT GGC CCG ACT CTG ACA ATT CAG-3′, and cfms-3360R, 5′-AGT GAA GGT CAA GAG TGG TGG CCA ATA ATG-3′. These primers were synthesized and submitted to Genome Systems (St Louis, MO) to screen a 129Sv mouse-derived embryonic stem (ES) cell genomic P1 library. Three genomic clones containing the *Csf1r* gene were obtained. One of these clones was mapped by a combination of restriction enzyme digestion, field inversion gel electrophoresis, Southern analyses, polymerase chain reaction (PCR), and sequencing. A 12-kb *Ase*I fragment spanning exons 2 to 6 was subcloned into the *Sma*I site in the multiple cloning site of pGEM7Z in which the *Apa*I site had been mutated, and the subclone was designated pGEM-Ase-Csf1r. The *Ase*I fragment was subjected to restriction enzyme mapping, PCR, and DNA sequencing to generate the restriction map shown in Figure 1A. A humanized green fluorescent protein (hGFP) sequence and the neomycin resistance (PGK-neo) cassette was cloned in-frame into the *Apa*I site in the exon 3 of pGEM-Ase-Csf1r, and a PGK-tk (thymidine kinase) cassette was cloned into the *Cla*I site in the multiple cloning site of the pGEM-Ase-Csf1r, yielding the final targeting vector (Figure 1A). A unique *Mlu*I site in the vector was used for linearization.

ES cell culture and chimeric mouse production

Mouse ES cells (Go Germline; Genome System) (ESVJ-1182) derived from 129SvJ strain were cultured on feeder layers of mitomycin C–treated mouse embryonic fibroblasts (MEFs) in ES cell medium (Dulbecco modified Eagle medium containing leukemia inhibitory factor [LIF]; Gibco BRL, Rockville, MD) at 37°C and 7.5% CO_2. MEF preparation, ES cell propagation, electroporation, and selection of recombinants with G418 and gancyclovir (Ganc) were carried out exactly as described in the Genome Systems manual. Briefly, ES cells were expanded on MEF feeder layers; after trypsinization and preplating to remove MEF, 1×10^7 ES cells were electroporated with 20 μg of the *Mlu*I-linearized targeting vector DNA. Twenty-four hours later, G418 and Ganc were added into the LIF-containing ES cell medium for selection over 6 days. $G418^r$/$Ganc^r$ ES clones were then picked and replated onto gelatinized 24-well plates in ES cell medium. After a further 2 days, the ES cells were trypsinized and split in 2, one half being used to expand cells for DNA extraction and the other half cultured for 2 further days before freezing. Genomic DNA was extracted from the expanded cells, digested with *Hin*dIII, and subjected to Southern blotting with an intron 7 probe to flanking sequence not included in the targeting vector to identify the targeted clones. The correctly targeted allele yielded an 8-kb *Hin*dIII band that was clearly resolved from a 7-kb band derived from the wild-type allele (Figure 1B). In addition, PCR products of the correctly targeted gene were obtained with forward and reverse primers corresponding to 5′ and 3′ sequences flanking the targeting vector sequence that were used respectively with reverse and forward primers within the 5′ and 3′ regions of the targeting vector. Selected clones bearing the correctly targeted allele were thawed, expanded, and injected into C57BL/6-derived blastocysts, which were transplanted into CD1 pseudopregnant females to generate chimeric founder mice. Subsequent genotyping of mice was carried out by PCR of tail DNA using the primers P1, P2 (wild-type allele) and P3, P4 (targeted allele) (Figure 1A). Primers P1 (5′-TCT CCT GGG ATG GGA AAC GAT CCC AAA GGC-3′) and P2 (5′-GAT TCA GGG TCC AAG GTC CAG ATG GGA GAG-3′) yielded a 536–base pair (bp) product, exclusively from the wild type allele, whereas P3 (5′-GCC AGC CAC GAT AGC CGC GCT GCC TCG TC-3′) and P4 (5′-CTT CCT GGC CCT CAA CCA CTG TCA C-3′) gave rise to a 1.6-kb product exclusively from the targeted allele.

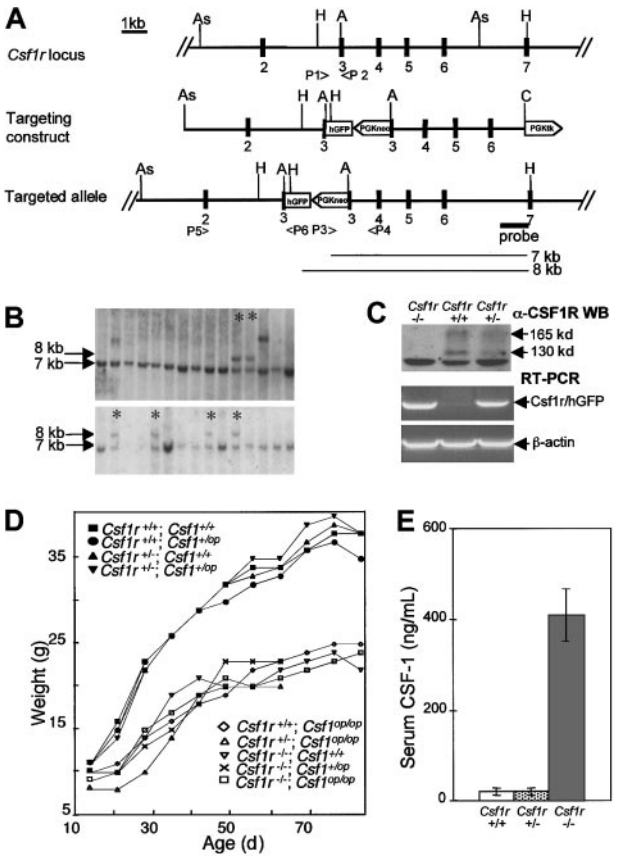

Figure 1. Targeted disruption of the mouse *Csf1r* gene: decreased growth rate and increased circulating CSF-1 in *Csf1r*$^{-}$/*Csf1r*$^{-}$ mice. (A) The targeted region of the *Csf1r* gene, the *Csf1r* gene-targeting vector, and the correctly targeted allele, showing exons 1 to 7, restriction enzyme sites (As, *Ase*I; H, *Hin*d III; A, *Apa*I; C, *Cla*I), PCR primers used (P1-P6, see text), the in-frame humanized green fluorescent protein (hGFP) sequence and the neomycin resistance (PGKneo) and thymidine kinase (PGKtk) cassettes above the flanking intron 7 probe were used to identify the 7-kb wild-type allele and 8-kb targeted allele *Hin*d III fragments depicted below it. (B) Southern blot analyses of the DNA from individual G418 and gancyclovir-resistant ES cell clones using the probe shown in A. Asterisks mark clones possessing the correctly targeted allele. (C) Anti–CSF-1R Western blot analysis of BMM (upper panel). The molecular masses of the mature CSF-1R (165 kDa) and its precursor (130 kDa) are indicated. RT-PCR of BMM RNA with primers P5, P6 (A) specific for the targeted allele (middle panel) and control primers for β-actin (lower panel) are shown. (D) Growth curves of progeny of double heterozygote (*Csf1r*$^{+}$/*Csf1r*$^{-}$;*Csf1*$^{+}$/*Csf1*^{op} × *Csf1r*$^{+}$/*Csf1r*$^{-}$;*Csf1*$^{+}$/*Csf1*^{op}) crosses (n ≥ 5 for each genotype). (E) Serum CSF-1 concentration determined by a radioimmunoassay that selectively detects biologically active CSF-1 (± SD; n ≥ 5 for each genotype).

Mice

To obtain germline transmission, chimeras were mated with C57BL/6J × C3Heb/FeJ-a/a strain mice on which the *Csf1*^{op} allele was maintained. All mice were maintained on this segregating background, behind a barrier at the Albert Einstein College of Medicine animal facility. *Csf1r*$^{-}$/*Csf1*$^{-}$ and *Csf1*^{op}/*Csf1*^{op} mice were distinguished from normal siblings at 10 days of age by the absence of incisor eruption and were fed ad libitum a powdered mixture of mouse food and infant milk formula (Enfamil) daily to improve their nutritional status. Control mice received mouse chow ad libitum. Genotyping of the *Csf1*^{op} allele was carried out as described.[37]

Radiographic analysis of mouse skeletal structure and CSF-1 radioimmunoassay

Radiographs were produced by exposing euthanized or anesthetized mice in a Faxitron pathology specimen x-ray cabinet (Faxitron X-Ray, Buffalo

Grove, IL). The animals were posed immediately above a fine-grained Polaroid 665 instant negative film package. Exposure was set at 50 kV for 1.5 minutes. The negatives were developed and printed according to the manufacturer's instructions (Polaroid, Cambridge, MA). CSF-1 in mouse sera was determined by a radioimmunoassay that selectively detects biologically active CSF-1.[38,39]

Immunohistochemistry and histochemistry

Rat monoclonal antibody to F4/80 was a gift from Dr David Hume (Department of Microbiology, University of Queensland). For immunostaining with F4/80 antibodies and histochemical localization of tartrate-resistant acid phosphatase (TRAP), siblings of the different genotypes were perfused and tissues were fixed, decalcified (knee joint only), embedded, sectioned, and immunostained as described.[2,40] TRAP staining was carried out as described.[40] Quantitative histomorphometric analyses of the hematoxylin and eosin–stained sections were performed using a digital camera to capture images. Image analysis was performed by using Image-Pro Plus (Media Cybernetics, Silver Spring, MD). F4/80$^+$ cells in tissue sections of at least 2 mice of a particular genotype at each age were quantitated as described.[2] Whole-mount preparations of the 4th inguinal mammary gland were stained with alum carmine as described.[41] For the estrus cycle analyses, daily vaginal smears were stained with hematoxylin and eosin. Mice were assessed as being in one of the 4 stages: proestrus (100% intact live epithelial cells), estrus (100% cornified epithelial cells), metestrus (50% cornified epithelial cells and 50% leukocytes), or diestrus (80%-100% leukocytes).[42]

Hematologic analysis and hematopoietic progenitor cell assays

Mice (6- to 8-week-old) were euthanized by exposure to a high concentration of CO_2. Blood was collected in heparinized tubes. Total white blood cells were counted in 6% CH_3COOH by using a hemocytometer. Red cell parameters were analyzed by using an automatic blood cell counter. Monocytes, granulocytes, and lymphocytes were resolved by differential flow cytometry analysis as described.[43] Spleen and bone marrow cell suspensions were assayed for high-proliferative potential colony-forming cells (HPP-CFCs) and CSF-1–dependent colony-forming units (CFU-Cs) in agar cultures as previously described.[31] Erythroid burst-forming unit (BFU-E) and granulocyte, erythroid, megakaryocyte, and macrophage colony-forming unit (CFU-GEMM) assays were performed by using reagents supplied by Stem Cell Technology (Vancouver, BC, Canada) in methylcellulose cultures as described by the manufacturers. The growth factors used for HPP-CFC agar cultures were stem cell factor, interleukin-6 (IL-6), IL-3, and granulocyte-macrophage CSF (GM-CSF). CFU-GEMM assays were performed in methylcellulose culture medium containing stem cell factor, IL-6, IL-3, and EPO.

Reverse transcriptase–PCR and Western blot

To assess *Csf1r* gene expression, bone marrow–derived macrophages (BMMs) were prepared from siblings of the different genotypes as previously described[44] but with GM-CSF replacing CSF-1. BMM cultured in mouse GM-CSF (R & D Systems, MN) was solubilized in sodium dodecyl sulfate–polyacrylamide gel electrophoresis (SDS-PAGE) running buffer,[45] subjected to SDS-PAGE, and Western blotted with a 1:1 mixture of 2 affinity purified goat antimouse CSF-1R cytoplasmic domain peptide antibodies.[46] Total RNA samples were prepared from BMM using the Trizol reagent (Gibco) and assayed by reverse transcriptase (RT)–PCR with primers that bind to exon 2 of the *Csf1r* gene and 5′ coding sequence of the GFP gene (P5 and P6, Figure 1A; P5 [5′-CTAGCAGCTGGGAGCCCCGTGCCCAGCCGACTC-3′]; P6 [5′-GGGTAGCGGCTGAAGCACTGCACGCCGTAGGTC-3′]). RT-PCR was carried out with an Advantage one-step RT-PCR kit (Clontech, Palo Alto, CA).

Statistical analyses

The mean, SD, or SEM of all numeric data was calculated. Data were analyzed by either Student *t* test or chi-square test, where appropriate. Comparisons of data sets yielding $P > .05$ were considered as not statistically significant.

Results

Targeted disruption of the mouse CSF-1R gene

A P1 clone containing the entire coding region and flanking DNA of CSF-1R gene was used to prepare the targeting construct (Figure 1A) as described in "Materials and methods." This vector was linearized and electroporated into 129SvJ strain ES cells, and clones of transfected cells resistant to both G418 and Ganc were screened for homologous recombinants by Southern blotting and PCR (Figure 1B). Of the 164 G418/Ganc-resistant clones obtained, 20 were identified as homologous recombinants and 2 of these (2C5 and 6D3) were injected into blastocysts. Of the 5 chimeras obtained, 3 (2 derived from 6D3 and one from 2C5) were transmitted to the germline. These lines were maintained on the same C57BL/6J × C3Heb/FeJ-a/a background as the *Csf1*^{op}/*Csf1*^{op} mice. Western blot analysis of whole cell lysates of BMM prepared from *Csf1r*$^-$/*Csf1r*$^-$ and littermate control mice indicated that the *Csf1r*$^-$/*Csf1r*$^-$ cells were devoid of CSF-1R (Figure 1C, top panel). Consistent with these results, RT-PCR analysis using primers P5 and P6 (Figure 1A) indicated that both *Csf1r*$^-$/*Csf1r*$^-$ and *Csf1r*$^+$/*Csf1r*$^-$ cells expressed mRNA encoding the CSF-1R–hGFP fusion protein (Figure 1C, lower panels). However, no significant expression of GFP could be detected in *Csf1r*$^-$/*Csf1r*$^-$ or *Csf1r*$^+$/*Csf1r*$^-$ cells by fluorescence microscopy or flow cytometry (data not shown).

Gross phenotype of *Csf1r*$^-$/*Csf1r*$^-$ mice

Csf1r$^-$/*Csf1r*$^-$ mice were identical in appearance to *Csf1*^{op}/*Csf1*^{op} mice. They were small (see below) and toothless and possessed truncated limbs, a domed skull, and, occasionally, a kinked tail. Studies with *Csf1*^{op}/*Csf1*^{op} mice indicate that they have a low body weight and a low growth rate.[28,37] Mice homozygous for the *Csf1*^{op} or *Csf1r*$^-$ mutations possessed a significantly lower growth rate and lower adult weight than double-positive control mice or mice heterozygous for the mutations and were indistinguishable from each other in this respect (Figure 1D). Furthermore, the growth curves of the double mutants were indistinguishable from those of mice homozygous for either mutation. The *Csf1r*$^-$/*Csf1r*$^-$ mice, like *Csf1*^{op}/*Csf1*^{op} mice,[47] were also deaf (data not shown).

A comparison of the genotypic frequencies for single heterozygous crosses (*Csf1*$^+$/*Csf1*^{op} × *Csf1*$^+$/*Csf1*^{op} and *Csf1r*$^+$/*Csf1r*$^-$ × *Csf1r*$^+$/*Csf1r*$^-$) is presented in Table 1. At birth, the frequency of the progeny of *Csf1*^{op} heterozygote and *Csf1r*$^-$ heterozygote crosses was as expected for a nondeleterious gene inherited in a Mendelian fashion. By weaning, however, the survival of *Csf1r*$^-$/*Csf1r*$^-$ mice approximated the survival of *Csf1*^{op}/*Csf1*^{op} mice, and the survival of both mutant mice was significantly lower than the survival of wild-type mice, as previously reported for *Csf1*^{op}/*Csf1*^{op} mice.[28] Analysis of the data from double heterozygote crosses at weaning (Table 2) revealed that survival of *Csf1*^{op}/*Csf1*^{op} mice was not significantly different from the survival of *Csf1r*$^-$/*Csf1r*$^-$ mice or of double mutant *Csf1*^{op}/*Csf1*^{op};*Csf1r*$^-$/*Csf1r*$^-$, except for the survival of *Csf1*^{op}/*Csf1*^{op};*Csf1r*$^+$/*Csf1r*$^-$ mice, which unexpectedly exhibited normal survival, suggesting that the *Csf1*^{op}/*Csf1*^{op} phenotype might be slightly less severe than the *Csf1r*$^-$/*Csf1r*$^-$ phenotype.

Previous studies from our laboratory indicated that 95% of the circulating CSF-1 is cleared by CSF-1R–mediated endocytosis and intracellular destruction by sinusoidally located macrophages and

Table 1. Frequency of genotypes of progeny of single heterozygote crosses of *Csf1^op^* and *Csf1r^−^* mutations

Age of progeny	Cross	Total progeny	Homozygous wild type	Heterozygotes	Homozygous mutant	χ^2 test probability*
1 d	*Csf1*$^+$/*Csf1*^{op} × *Csf1*$^+$/*Csf1*^{op}	40	12 (1.2)†	17 (1.7)	11 (1.1)	0.62
	Csf1r$^+$/*Csf1r*$^-$ × *Csf1r*$^+$/*Csf1r*$^-$	72	21 (1.17)	38 (2.11)	13 (0.72)	0.37
3 wk	*Csf1*$^+$/*Csf1*^{op} × *Csf1*$^+$/*Csf1*^{op}	214	71 (1.32)	109 (2.04)	34 (0.64)	0.002
	Csf1r$^+$/*Csf1r*$^-$ × *Csf1r*$^+$/*Csf1r*$^-$	393	107 (1.09)	221 (2.24)	65 (0.66)	0.005

*Probability that results do not differ significantly from the 1:2:1 ratio.
†Ratio compared with expected 1:2:1 ratio of an independently segregating gene.

that circulating CSF-1 has a half-life of only 10 minutes.[48] We therefore determined the CSF-1 concentration in the sera of *Csf1r^−^/Csf1r^−^*, *Csf1r^+^/Csf1r^+^*, and *Csf1r^+^/Csf1r^−^* mice (Figure 1E). Consistent with these previous observations, levels of serum CSF-1 in *Csf1r^−^/Csf1r^−^* mice were elevated approximately 20-fold compared with the levels in *Csf1r^+^/Csf1r^+^* littermate control mice. Interestingly, the levels of circulating CSF-1 in the *Csf1r^+^/Csf1r^−^* mice (19.0 ± 5.4 ng/mL) were within normal range (19.9 ± 6.1 ng/mL).

Comparison of the osteopetrotic phenotypes of *Csf1r^−^/Csf1r^−^* and *Csf1^op^/Csf1^op^* mice

*Csf1^op^/Csf1^op^* mice exhibit impaired bone resorption associated with a reduction in the number of osteoclasts.[28] Their inability to remodel bone resulted in general skeletal deformities that, as shown in Figure 2, were shared with the *Csf1r^−^/Csf1r^−^* mice. Compared with wild-type littermates, the long bones of their limbs were short (Figure 2) with increased bone density at the metaphyses (Figure 2), deformities in the flat bony plates result in a domed skull (Figure 2), and the increased bone density in the mandible presumably leads to the failure of tooth eruption (Figure 2). Interestingly, a radiograph analysis of the temporal changes in the femurs of wild-type and mutant mice with age (Figure 2) indicates that there is significantly more radiopacity in the distal metaphysis of the femurs of *Csf1r^−^/Csf1r^−^* than of *Csf1^op^/Csf1^op^* mice. Similar results were obtained with *Csf1r^−^/Csf1r^−^* mice derived from both 2C5 and 6D3 ES cell lines. All further experiments were carried out with *Csf1r^−^/Csf1r^−^* mice derived from 2C5 ES cells.

The metaphyseal radiopacity of the long bones of *Csf1^op^/Csf1^op^* and *Csf1r^−^/Csf1r^−^* mice is the result of the failure of osteoclast development at this site. Hematoxylin and eosin staining of longitudinal sections of the distal metaphyseal regions of the femurs of these mice revealed that both *Csf1r^−^/Csf1r^−^* and *Csf1^op^/Csf1^op^* mice possessed higher amounts of bony trabeculae than littermate control mice, consistent with impaired bone remodeling (Figure 3A). In addition, TRAP$^+$ cells (osteoclasts) were present in low numbers in the bony trabecula regions of *Csf1^op^/Csf1^op^* femurs compared with littermate control femurs and even fewer in number in *Csf1r^−^/Csf1r^−^* femurs (Figure 3B). Histomorphometric analyses of the entire bone marrow cavity of the femurs were consistent with these observations, the percentage of trabecular bone in *Csf1r^−^/Csf1r^−^* and *Csf1^op^/Csf1^op^* femurs being greater than in wild-type femurs (Figure 3C). In the metaphyseal region, the retention of trabecular bone was greater for *Csf1r^−^/Csf1r^−^* (92%) than for *Csf1^op^/Csf1^op^* (83%) mice (compared with wild-type

Table 2. Genotypic frequencies as a percentage of total 3-week-old progeny from double heterozygote (*Csf1r^+^/Csf1r^−^; Csf1^+^/Csf1^op^* × *Csf1r^+^/Csf1r^−^; Csf1^+^/Csf1^op^*) crosses

	Csf1r genotype		
Csf1 genotype	*Csf1r*$^+$/*Csf1r*$^+$	*Csf1r*$^+$/*Csf1r*$^-$	*Csf1r*$^-$/*Csf1r*$^-$
Csf1$^+$/*Csf1*$^+$	6.25/7.7*	12.5/17.6	6.25/3.8
Csf1$^+$/*Csf1*^{op}	12.5/15.3	25.0/31.0	12.5/4.2
Csf1^{op}/*Csf1*^{op}	6.25/4.2	12.5/12.6	6.25/3.4

*Percentage expected for independently segregating alleles/percentage observed, n = 261.

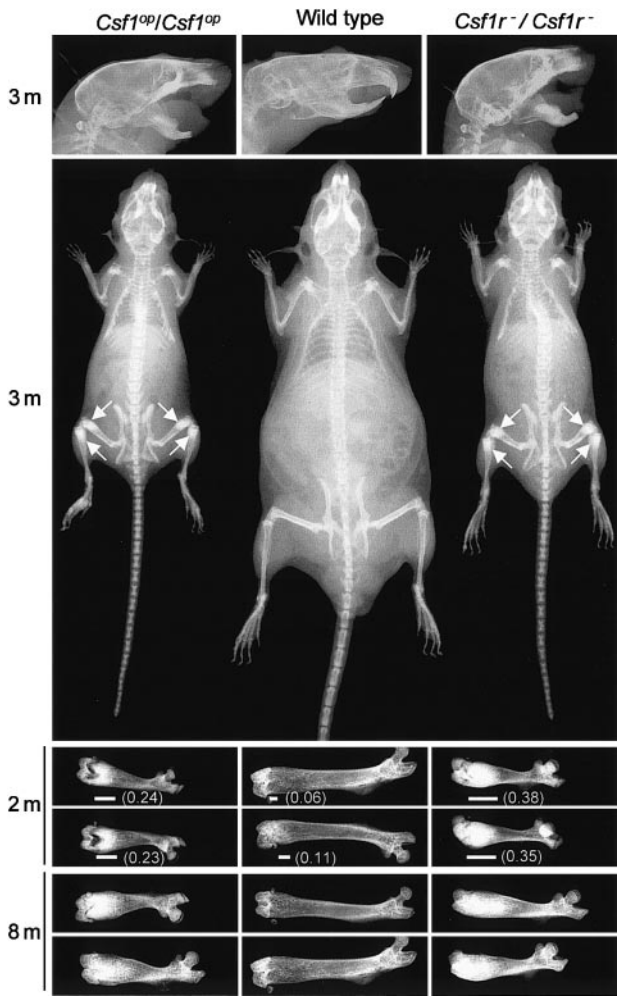

Figure 2. Comparison of the skeletal development of wild-type, *Csf1^op^/Csf1^op^*, and *Csf1r^−^/Csf1r^−^* mice. Radiograms of the heads, bodies, and femurs of mice of the indicated genotypes at different ages (m, months). Each femur is from a different mouse. Arrows indicate regions of increased bone density most easily visualized at this magnification. Also shown is the extent (horizontal line) and fraction (in parenthesis) of the total femur length that is of high radiopacity.

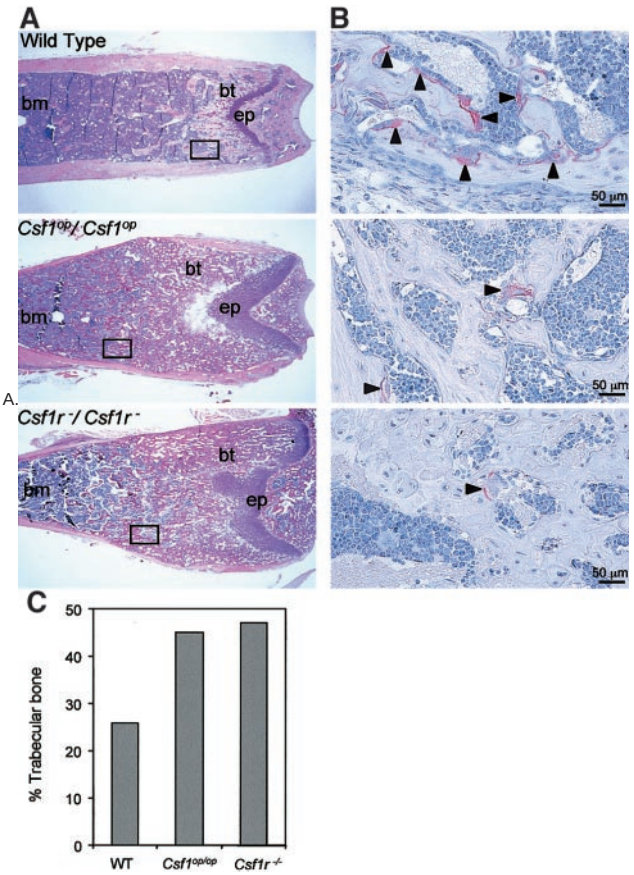

Figure 3. Histology of bone marrow of wild type, *Csf1*^{op}/*Csf1*^{op}, and *Csf1r*$^{-}$/*Csf1r*$^{-}$ mice. (A) Low-power photomicrographs of hematoxylin and eosin–stained midsagittal 5-μm sections of the distal femoral metaphyses of 8-week-old mice (bm, bone marrow; bt, bony trabeculae; ep, epiphyseal plate). Boxes indicate comparable areas of TRAP-stained sections photographed in B. (B) High-power photomicrographs of TRAP staining for osteoclasts in midsagittal 5-μm sections of femurs of 4-week-old mice in areas comparable to those boxed in A. Counterstained with hematoxylin. Arrowheads indicate TRAP^{+} cells. (C) Percentage of trabecular bone in the entire bone marrow cavity determined from the sections used in A. Original magnification A, × 25; B, × 400.

mice [43%]), reflecting the greater radiopacity of the *Csf1r*$^{-}$/*Csf1r*$^{-}$ over *Csf1*^{op}/*Csf1*^{op} femurs in this region (Figure 2).

Consequent to their decreased volume of femoral bone marrow, the total femoral marrow cellularity of *Csf1*^{op}/*Csf1*^{op} and *Csf1r*$^{-}$/*Csf1r*$^{-}$ mice was significantly lower than the bone marrow cellularity of wild-type mice (Table 3). As previously reported for *Csf1*^{op}/*Csf1*^{op} mice,[31,32] the bone marrow cellularity *Csf1r*$^{-}$/*Csf1r*$^{-}$ mice recovered to the levels observed in control wild type mice by 8 months of age (Table 3), despite evidence of some residual osteopetrosis in both *Csf1*^{op}/*Csf1*^{op} and *Csf1r*$^{-}$/*Csf1r*$^{-}$ mice (Figure 2).

Reduced mononuclear phagocyte production in *Csf1r*$^{-}$/*Csf1r*$^{-}$ mice

Previous reports[34,49] have shown that blood monocyte and lymphocyte percentages are reduced in *Csf1*^{op}/*Csf1*^{op} mice. Fluorescence-activated cell sorter (FACS) analysis of these populations by forward and side-light scatter revealed that there was a decrease in monocytes and lymphocytes and an increase in granulocytes in the circulation of *Csf1r*$^{-}$/*Csf1r*$^{-}$ mice and that they were not significantly different from *Csf1*^{op}/*Csf1*^{op} mice in this respect (Figure 4A). Similarly, the total cellularities of the pleural and peritoneal cavities of *Csf1r*$^{-}$/*Csf1r*$^{-}$ mice were reduced to the same extent as in *Csf1*^{op}/*Csf1*^{op} mice (Figure 4B) as were the frequencies of Mac1(CD11b)$^{+}$ cells in these cavities (Figure 4C). Tissue macrophages expressing macrophage-specific cell-surface protein, F4/80, are significantly decreased in many tissues of *Csf1*^{op}/*Csf1*^{op} mice.[2] The F4/80^{+} cell densities of several such tissues were determined in wild-type, *Csf1*^{op}/*Csf1*^{op}, and *Csf1r*$^{-}$/*Csf1r*$^{-}$ mice at ages in which the F4/80^{+} macrophage density had previously been shown[2] to be maximum for the particular wild-type tissue (Figure 5, Table 4).[2,50,51] As previously shown,[2] the F4/80^{+} cell densities of the tissues of *Csf1*^{op}/*Csf1*^{op} mice were significantly lower than those of wild-type control mice (including the Langerhans cells of the epidermis, previously reported to be normal in *Csf1*^{op}/*Csf1*^{op}

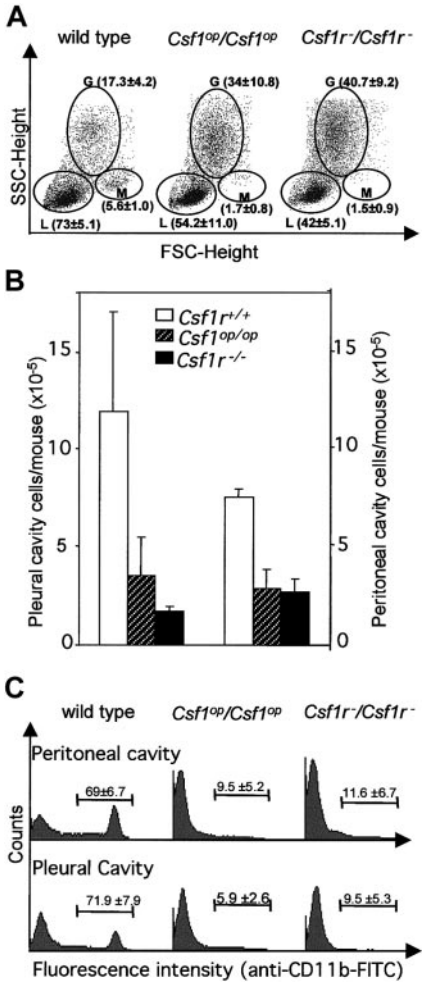

Figure 4. FACS analysis of blood leukocytes, peritoneal cavity, and pleural cavity cells. (A) Typical FACS analyses of monocytes, granulocytes, and lymphocytes by forward and side light scatter. Separate regions encompassing the monocyte (M), granulocyte (G), and lymphocyte (L) subpopulations are indicated. The means of results of such analyses for 3 mice of each genotype are shown in brackets (± SD). (B) Total pleural cavity and peritoneal cavity cells (n = 3). (C) Typical FACS analyses of CD11b^{+} peritoneal and pleural cavity cells. Percentage of positive cells for 3 mice of each genotype (± SD) is shown within each FACS distribution. FITC indicates fluorescein isothiocyanate; FSC, forward scatter; SSC, side scatter.

Table 3. Bone marrow cellularity of 7-week-old and 8-month-old mice

	Total femur cellularity/body weight (×10^{-6}/g)		
Age	Wild type	*Csf1*^{op}/*Csf1*^{op}	*Csf1r*$^{-}$/*Csf1r*$^{-}$
7 wk	0.50 ± 0.10	0.25 ± 0.04*	0.23 ± 0.10*
8 mo	1.57 ± 0.28	1.90 ± 0.14	1.53 ± 0.82

*Significantly different from wild type (Student *t* test $P \leq .01$).

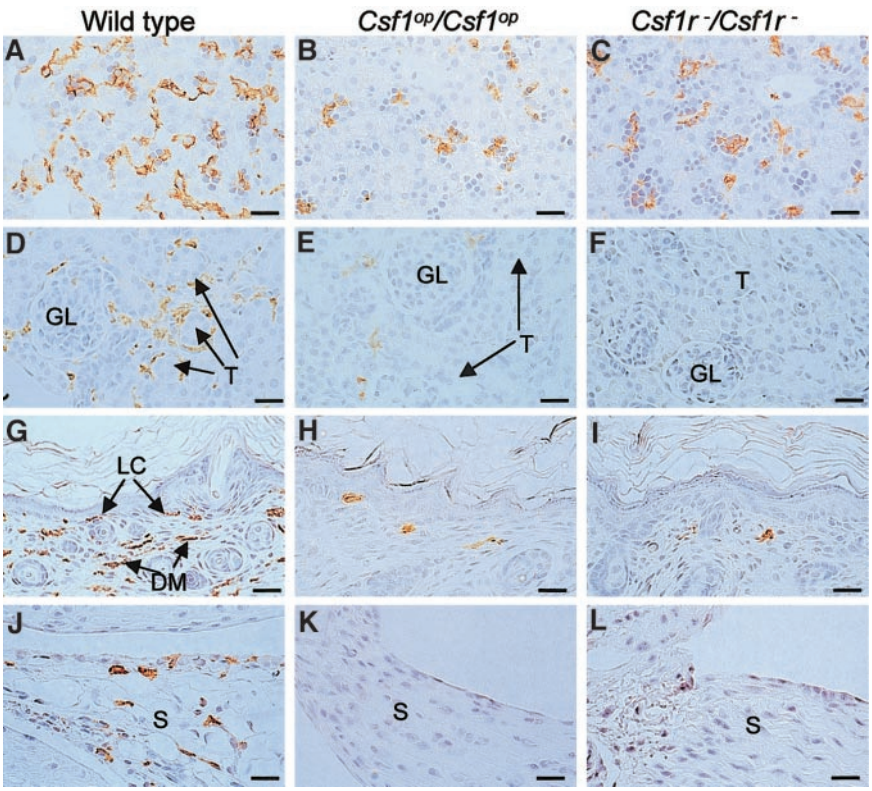

Figure 5. F4/80$^+$ cells in liver, kidney, skin, and synovial membrane. Tissues from wild-type, *Csf1^{op}/Csf1^{op}*, and *Csf1r$^-$/Csf1r$^-$* mice were immunostained with a monoclonal antibody to F4/80 that selectively stains macrophages and were counterstained with hematoxylin. Sections of (A-C) 2-day-old livers, (D-E) 2-week-old kidneys showing macrophages surrounding the glomeruli (GL) and tubules (T) of wild-type mice (D), (F-I) 2-day-old skin showing immunostaining of both Langerhans cells (LC) and dermal macrophages (DM) from wild-type mice, and (J-L) longitudinal sections of 2-week-old knee joints in the region of the synovial membrane (S) showing immunostaining of cells in the wild-type synovial membranes. Note the more rounded and less dendritic appearance of the F4/80$^+$ cells in the tissues of the *Csf1^{op}/Csf1^{op}* and *Csf1r$^-$/Csf1r$^-$* mice, previously reported for *Csf1^{op}/Csf1^{op}* mice. Bar, 50 μm. Original magnification A-L, × 400.

mice[2]). There was no difference between the lowered F4/80$^+$ cell densities of these tissues and those of *Csf1r$^-$/Csf1r$^-$* mice, except that the F4/80$^+$ cell density in the kidney was significantly lower in *Csf1r$^-$/Csf1r$^-$* mice than in *Csf1^{op}/Csf1^{op}* mice (Table 4). Thus, apart from this difference, the mononuclear phagocyte numbers were equivalently reduced in *Csf1r$^-$/Csf1r$^-$* and *Csf1^{op}/Csf1^{op}* mice.

Hematopoietic progenitor cells in *Csf1r$^-$/Csf1r$^-$* mice

Previous experiments have shown that, consistent with their reduced space for marrow hematopoiesis (Table 3, Figures 2 and 3), 6-week-old *Csf1^{op}/Csf1^{op}* mice have a compensatory splenic hematopoiesis with elevated frequencies of CFU-Cs and HPP-CFCs.[31] As in the case of the *Csf1^{op}/Csf1^{op}* mice (3.6 ± 0.2), the splenic weights (milligram per gram of body weight) of 6-week-old *Csf1r$^-$/Csf1r$^-$* mice (5.1 ± 0.5) were significantly elevated compared with those of littermate control wild-type mice (3.0 ± 0.3 [± SD], n = 3). The hematopoietic status of the wild-type, *Csf1^{op}/Csf1^{op}*, and *Csf1r$^-$/Csf1r$^-$* mice was examined by determining bone marrow and splenic frequency of hematopoietic progenitor cells at 6 weeks of age (Figure 6). Splenic BFU-Es and HPP-CFCs were elevated to a similar extent in both types of mutant mouse. There was no significant effect of either mutation on CFU-GM or CFU-GEMM. As expected, in contrast to the elevated frequency of CSF-1–responsive splenic CFU-C in the *Csf1^{op}/Csf1^{op}* mice, there were no CSF-1–responsive progenitors in spleens of the *Csf1r$^-$/Csf1r$^-$* mice. In the bone marrow of both *Csf1^{op}/Csf1^{op}* and *Csf1r$^-$/Csf1r$^-$* mice, there was no difference in the frequency of these progenitors compared with their frequency in wild-type mice, save for the absence of CFU-Cs in the *Csf1r$^-$/Csf1r$^-$* mice. These results reflect a negative regulatory role of CSF-1 on the in vivo frequencies of splenic BFU-Es and HPP-CFCs.

Table 4. Tissue F4/80$^+$ cell densities

Tissue	Age of mice	Wild type	*Csf1^{op}/Csf1^{op}*	*Csf1r$^-$/Csf1r$^-$*
Bone marrow*†	2 wk	697.7 ± 11.7	210.5 ± 14.8	173.7 ± 41.0
Liver*†	2 d	678.1 ± 108.4	413.4 ± 13.0	463.7 ± 45.3
Liver*†	4 mo	372.9 ± 44.2	124.3 ± 7.2	150.0 ± 68.2
Kidney*†‡	2 wk	184.3 ± 83.0	34.5 ± 1.6	12.3 ± 0.4
Thymus*†	2 wk	376.4 ± 40.1	110.6 ± 18.1	168.3 ± 15.2
Langerhans cells*†	2 d	15.8 ± 1.3§	3.0 ± 1.4§	2.0 ± 1.4§
Dermis*†	2 d	253.1 ± 56.0	15.4 ± 5.1	32.5 ± 10.0
Testes*†	2 wk	178.3 ± 83.2	46.7 ± 22.2	34.6 ± 19.4

Densities in cells/mm^2 average of multiple counts (±SD, n = 4) of tissue sections from at least 2 mice per genotype.

*Significant differences between wild type and *Csf1^{op}/Csf1^{op}* ($P \leq .05$).

†Significant differences between wild type and *Csf1r$^-$/Csf1r$^-$* ($P \leq .05$).

‡Significant differences between *Csf1^{op}/Csf1^{op}* and *Csf1r$^-$/Csf1r$^-$* ($P \leq .05$).

§Densities in cells/mm average of multiple counts (±SD, n = 4) of tissue sections from at least 2 mice per genotype.

Reproductive phenotype of *Csf1r$^-$/Csf1r$^-$* mice

CSF-1 plays an important role in ovulation, preimplantation, placental function, regulation of the estrous cycle, and lactation.[3,4,52-55] Estrous cycling times are altered in mature *Csf1^{op}/Csf1^{op}* mice, estrous occurring irregularly and more infrequently compared with the estrous times of normal mice (~5 days).[53] The duration of estrous in female *Csf1r$^-$/Csf1r$^-$* mice, determined by the appearance in the vagina of exfoliated anuclear cornified cells and the absence of macrophages, although lower (8.0 ± 2.0, n = 40; Figure 7A) than the previously reported cycling time for *Csf1^{op}/Csf1^{op}* mice (~14.5 days), was significantly higher than the duration of estrus in wild-type mice (5.9 ± 0.5, n = 40; Figure 7 A). As previously reported for the *Csf1^{op}/Csf1^{op}* mice, this increase in cycling time was primarily due to an increase in the duration of the diestrus period (Figure 7B). In pregnant *Csf1^{op}/Csf1^{op}* mice, the lactating mammary gland fails to develop normally because of a

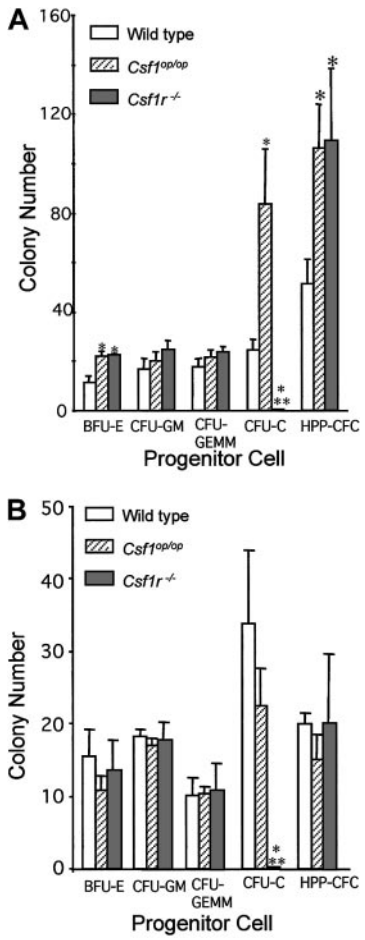

Figure 6. Hematopoietic progenitor cell concentrations in the spleen and bone marrow of 6-week-old mice. (A) Splenic progenitor cell colony numbers per 10^5 cells (BFU-E, CFU-GM, CFU-GEMM, CFU-C) or per 10^4 cells (HPP-CFC). (B) Bone marrow progenitor cell colony numbers per 10^4 cells (BFU-E, CFU-GM, CFU-GEMM, CFU-C) or per 10^3 cells (HPP-CFC). Means ± SD (3 mice per genotype). *Significantly different from wild type; **Significantly different from wild type and *Csf1^{op}/Csf1^{op}* ($P \leq .01$).

failure of branching morphogenesis of the ductal epithelium.[56] As shown in the whole-mount stained mammary glands in Figure 7C, a similar phenotype was observed for mammary glands from pregnant *Csf1r*$^{-}$/*Csf1r*$^{-}$ mice.

Compared with normal males, *Csf1^{op}/Csf1^{op}* male mice had low testosterone levels, low libido, and reduced viable sperm numbers, as well as mating infrequently and displaying a long latency between mating when presented serially with female mice in estrous.[42] A similar phenotype was observed for *Csf1r*$^{-}$/*Csf1r*$^{-}$ mice, which mated less frequently with cycling females and produced fewer pregnant females on successive days following daily exposure to different superovulated females than wild-type males (Figure 7D).

Discussion

In this study, we have shown that BMM from mice in which both *Csf1r* alleles have been targeted by the insertion of a PGKneo cassette containing stop codons into exon 3 fail to express detectable CSF-1R mRNA or protein. In contrast, BMM from wild-type mice express approximately 50 000 cell surface CSF-1R molecules per cell.[7] Consistent with this observation, neither bone marrow nor splenic cells from the *Csf1r*$^{-}$/*Csf1r*$^{-}$ mice are able to form CSF-1–dependent macrophage colonies in agar cultures. Furthermore, the circulating concentrations of CSF-1 in the *Csf1r*$^{-}$/*Csf1r*$^{-}$ mice were 20-fold higher than the wild-type CSF-1 concentration, consistent with a failure of the previously established, CSF-1R–mediated clearance mechanism for circulating CSF-1.[48] These results indicate that the *Csf1r*$^{-}$/*Csf1r*$^{-}$ mice are truly CSF-1R nullizygous.

The phenotype of the *Csf1r*$^{-}$/*Csf1r*$^{-}$ mice was very similar to the phenotype of the *Csf1^{op}/Csf1^{op}* mice lacking CSF-1. The growth rates and postnatal lethalities of *Csf1r*$^{-}$/*Csf1r*$^{-}$, *Csf1^{op}/Csf1^{op}*, and the double-mutant *Csf1r*$^{-}$/*Csf1r*$^{-}$;*Csf1^{op}/Csf1^{op}* mice are indistinguishable. Of interest was the demonstration that postnatal lethality of both mutants was not detectable at day 1 but became apparent by 3 weeks of age (Table 1). Both *Csf1r*$^{-}$/*Csf1r*$^{-}$ and *Csf1^{op}/Csf1^{op}* mice were toothless and severely osteopetrotic with the same osteopetrosis-associated skeletal abnormalities and with a reduced bone marrow cellularity that returns to normal levels by 8 months of age. There was a similar depletion of circulating monocytes, pleural and peritoneal cavity cells, peritoneal cavity Mac1^{+} cells, and tissue macrophages in both mutant mice. With the exception of CSF-1–dependent CFU-Cs, which cannot be measured in the *Csf1r*$^{-}$/*Csf1r*$^{-}$ mice, there was no difference in their levels of bone marrow hematopoietic progenitor cells, and both mutants had splenic BFU-E and HPP-CFC levels that were significantly higher than in wild-type control mice. Furthermore, both mutants shared previously reported defects in reproductive function, including longer estrus cycles, failure of normal lactating mammary gland development, and a reduced male mating performance. As no phenotype in the *Csf1^{op}/Csf1^{op}* mice

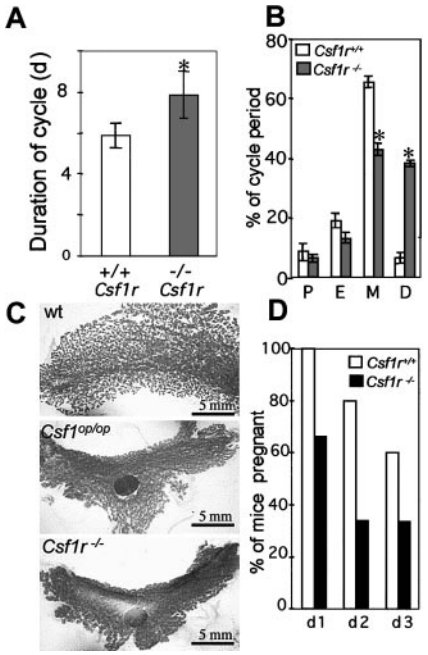

Figure 7. Reproductive phenotype of *Csf1r*$^{-}$/*Csf1r*$^{-}$ mice. (A) Duration of estrus cycle in virgin female mice (5 mice per genotype, 8 cycles/mouse, ± SD). (B) Percentage time in proestrus (P), in estrus (E), in metestrus (M), and in diestrus (D) (± SD). (C) Whole-mount alum-carmine staining of the 4th inguinal mammary gland from 18-day pregnant mice. All panels are at the same magnification, approximately only one third of the wild-type gland is shown. LN indicates lymph node. (D) Percentage of successful pregnancies resulting from the consecutive daily mating of wild-type (open) and *Csf1r*$^{-}$/*Csf1r*$^{-}$ (filled) male mice with superovulated virgin female mice. *Indicates significantly different from wild type; wt, wild type.

was more severe than in the *Csf1r*$^{-}$/*Csf1r*$^{-}$ mice, these results indicate that all of the effects of CSF-1 are mediated via the CSF-1R that is encoded by the c-*fms* gene.

Despite the overall similarity of the *Csf1r*$^{-}$/*Csf1r*$^{-}$ and *Csf1*^{op}/*Csf1*^{op} mouse phenotypes, aspects of the *Csf1r*$^{-}$/*Csf1r*$^{-}$ phenotype were more severe than those of the *Csf1*^{op}/*Csf1*^{op} mouse. These aspects include a slightly more severe osteopetrosis in the femurs (Figures 2 and 3) and a more severe depletion of F4/80^{+} cells in the kidney (Figure 5, Table 4). In addition, there was a difference in the postnatal survival of mice homozygous for one allele and heterozygous for the other. *Csf1*^{op}/*Csf1*^{op};*Csf1r*$^{+}$/*Csf1r*$^{-}$ mouse survival was as expected for 2 independently segregating alleles with no associated lethality, whereas the survival of *Csf1r*$^{-}$/*Csf1r*$^{-}$;*Csf1*$^{+}$/*Csf1*^{op} mice was one third that rate (Table 2). Because both *Csf1r*$^{+}$/*Csf1r*$^{+}$;*Csf1*^{op}/*Csf1*^{op} and *Csf1r*$^{-}$/*Csf1r*$^{-}$;*Csf1*$^{+}$/*Csf1*$^{+}$ mice also survived at one third of the expected rate, this finding suggests that a single copy of the CSF-1R gene may confer an advantage in the absence of CSF-1. This observation, with significant numbers of progeny, supports the concept of a CSF-1–independent protective effect of the CSF-1R, although it is not clear how 2 copies of the CSF-1R gene fail to protect. It is possible that some of these effects were due to partial rescue of the *Csf1*^{op}/*Csf1*^{op} mice by transplacental passage of CSF-1 from the heterozygotic mothers,[57] which is not possible in the case of the *Csf1r*$^{-}$/*Csf1r*$^{-}$ mice. However, because no difference was observed between the liver F4/80^{+} cell densities of 2-day-old *Csf1*^{op}/*Csf1*^{op} and *Csf1r*$^{-}$/*Csf1r*$^{-}$ mice and nearly 80% of the fetal hepatic blood flow is derived directly from the umbilical vein,[58] this seems unlikely. Furthermore, the increased severity of *Csf1r*$^{-}$/*Csf1r*$^{-}$ phenotype has recently been confirmed by using the progeny of mice of a single strain on which both alleles have been backcrossed for more than 5 generations. On this background, the *Csf1r*$^{-}$/*Csf1r*$^{-}$ phenotype is even more severe and the *Csf1r*$^{-}$/*Csf1r*$^{-}$ mice all die by 3 weeks of age, whereas the *Csf1*^{op}/*Csf1*^{op} survival approximates their survival on the C57BL/6J × C3Heb/FeJ-a/a background. These observations suggest that the CSF-1R can respond to an additional ligand or can function in a ligand-independent fashion in some situations.

It has previously been suggested, in part because of the residual tissue macrophage production seen in certain tissues in *Csf1*^{op}/*Csf1*^{op} mice and in part because of the nature of the mutation, that this mouse is not completely devoid of a mutated yet active form of CSF-1.[59] However, as indicated above, the *Csf1*^{op}/*Csf1*^{op} and *Csf1r*$^{-}$/*Csf1r*$^{-}$ phenotypes were very similar. In particular, with one exception, every *Csf1r*$^{-}$/*Csf1r*$^{-}$ tissue possessed macrophage concentrations that did not significantly differ from those of the corresponding *Csf1*^{op}/*Csf1*^{op} tissue. These observations strongly suggest that the residual tissue macrophage populations in *Csf1*^{op}/*Csf1*^{op} mice are not due to the action of a mutated less-efficient CSF-1. Thus, the present study indicates that other growth factors are involved in the regulation of macrophage production observed in *Csf1*^{op}/*Csf1*^{op} and *Csf1r*$^{-}$/*Csf1r*$^{-}$ mice. Among the known growth factors most likely to be responsible for macrophage production in these mutant mice are GM-CSF and IL-3 and vascular endothelial growth factor. GM-CSF and IL-3 together are capable of correcting not only the osteopetrotic condition of *Csf1*^{op}/*Csf1*^{op} mice but also macrophage deficiencies in several tissues.[60] Vascular endothelial growth factor is also able to correct the osteopetrotic condition of *Csf1*^{op}/*Csf1*^{op} mice and appears to be responsible for the age-related increase in osteoclasts in these mice.[33]

It has previously been reported that the percentage of blood monocytes and lymphocytes is reduced[34,37,49] and the percentage of blood granulocytes increased[37,49] in *Csf1*^{op}/*Csf1*^{op} mice, without significant changes in the circulating leukocyte concentration. These changes in monocytes and granulocytes are not unexpected, given the specificity of CSF-1 for the mononuclear phagocytic lineage[13,38] and the existence of progenitors capable of giving rise to both granulocytes and macrophages.[61] However, the decrease in the percentage of blood lymphocytes, which we also observed in both *Csf1*^{op}/*Csf1*^{op} and *Csf1r*$^{-}$/*Csf1r*$^{-}$ mice in the present study, is of interest. Recently, it has also been shown that the frequencies of stromal cell– and IL-7–dependent B-cell precursors and CFU–IL-7 in bone marrow were significantly diminished in *Csf1*^{op}/*Csf1*^{op} mice, as well as other osteopetrotic mice (*Fos*-nullizygous and *microphthalmia (Mitf*^{mi}/*Mitf*^{mi}*)*. However, these precursors could be generated from *Csf1*^{op}/*Csf1*^{op} bone marrow precursor cells on in vitro incubation with stromal cells in the presence of IL-7.[62] Also, CSF-1 has been shown to reduce apoptosis in precursor B cells in whole mouse bone marrow cultures but not in cultures of B220^{+} B-lineage cells, implying that CSF-1 can indirectly regulate B lymphopoiesis.[63] These results suggest that the decreased B lymphopoiesis in *Csf1*^{op}/*Csf1*^{op} mice results from alterations of the microenvironment rather than from a B-cell autonomous defect. The CSF-1R–nullizygous mice will be useful in analyzing direct and indirect effects of CSF-1 in B lymphopoiesis.

The development of the CSF-1R–nullizygous mouse permits new approaches to be taken to the analysis of CSF-1 action. In studies of CSF-1R signal transduction, a powerful approach to our understanding of CSF-1R structure-function has been to introduce mutated forms of the receptor into fibroblast or myeloid cell lines that do not express the CSF-1R.[64-68] However, the functions affected by particular CSF-1R mutations have been found to differ substantially, indicating the importance of cellular context for experiments of this kind (reviewed in Hamilton[69,70]). By using BMM and progenitor cells from *Csf1r*$^{-}$/*Csf1r*$^{-}$ mice and cell lines derived from them, as well as "knock-in" mutation approaches based on the "knock-out" construct used here, it is now possible to carry out these experiments in the correct cellular context.

Circulating CSF-1 is composed of both proteoglycan and glycoprotein forms.[71] The analysis of these forms and their regulation has been limited by the amounts of mouse serum needed and the low specific activity of serum CSF-1 per unit serum protein. The 20-fold elevation of the concentration (and specific activity) of serum CSF-1 in *Csf1r*$^{-}$/*Csf1r*$^{-}$ mice will greatly facilitate these investigations.

Perhaps the area of most immediate import is the assessment of the role of CSF-1 in the regulation of primitive hematopoietic cells. Previous studies have indicated that, although CFU-Cs are the most primitive cells that can be stimulated to proliferate and differentiate by CSF-1 alone in vitro, CSF-1 can cause the proliferation and differentiation of precursors of the CFU-Cs, by synergizing with other growth factors that alone have limited or no effect on the proliferation of the primitive cells.[10,11,27,72] Indeed, the observation in the present study that splenic BFU-E and HPP-CFC levels in *Csf1*^{op}/*Csf1*^{op} and *Csf1r*$^{-}$/*Csf1r*$^{-}$ mice are significantly elevated already suggests that CSF-1, via the CSF-1R, negatively regulates the maintenance of these precursor cells. Consistent with the observed elevation of BFU-Es and HPP-CFCs, CSF-1 has been shown to inhibit erythroid and erythroid/myeloid colony formation in vitro.[73] CSF-1 has also been shown to inhibit the differentiation of ES cells to blood cells other than macrophages.[74] In addition, it

has recently been shown that ectopic expression of the CSF-1R in the multipotent hematopoietic EML cell line decreases their erythroid potential,[75] raising the possibility that CSF-1R regulates erythroid differentiation and/or commitment. Because of the cell autonomous nature of the *Csf1r*$^{-}$ mutation, it is now possible to study the role of the receptor in the generation of primitive cells of different lineages by using bone marrow transplantation. Such an approach permits testing of CSF-1/CSF-1R regulation of cell proliferation and differentiation in the absence of an endogenous osteopetrotic condition.

Acknowledgments

We thank members of the AECOM analytical imaging, FACS, histopathology, hybridoma, and transgenic and gene targeting facilities for assistance in different aspects of the work; Dr Paula E. Cohen for advice on the fertility analysis; Dr Sandy C. Marks Jr for advice on TRAP staining; David Gebhard of the AECOM FACS facility for assistance with the FACS analyses; Dr Thomas Graf for reviewing the manuscript; and Xiao-Hua Zong for technical assistance.

References

1. Stanley ER. CSF-1. In: Oppenheim JJ, Feldmann M, eds. Cytokine Reference: a Compendium of Cytokines and Other Mediators of Host Defence. London, United Kingdom: Academic Press; 2000: 911-934.
2. Cecchini MG, Dominguez MG, Mocci S, et al. Role of colony stimulating factor-1 in the establishment and regulation of tissue macrophages during postnatal development of the mouse. Development. 1994;120:1357-1372.
3. Pollard JW, Stanley ER. Pleiotropic roles for CSF-1 in development defined by the mouse mutation osteopetrotic. Adv Dev Biochem. 1996;4: 153-193.
4. Cohen PE, Nishimura K, Zhu L, Pollard JW. Macrophages: important accessory cells for reproductive function. J Leuk Biol. 1999;66:765-772.
5. Guilbert LJ, Stanley ER. Specific interaction of murine colony-stimulating factor with mononuclear phagocytic cells. J Cell Biol. 1980;85:153-159.
6. Byrne PV, Guilbert LJ, Stanley ER. Distribution of cells bearing receptors for a colony-stimulating factor (CSF) in murine tissues. J Cell Biol. 1981; 91:848-853.
7. Guilbert LJ, Stanley ER. The interaction of ^{125}I-colony stimulating factor-1 with bone marrow-derived macrophages. J Biol Chem. 1986;261: 4024-4032.
8. Yeung Y-G, Jubinsky PT, Sengupta A, Yeung DC-Y, Stanley ER. Purification of the colony-stimulating factor 1 receptor and demonstration of its tyrosine kinase activity. Proc Natl Acad Sci U S A. 1987;84:1268-1271.
9. Sherr CJ, Rettenmier CW, Sacca R, Roussel MF, Look AT, Stanley ER. The c-fms proto-oncogene product is related to the receptor for the mononuclear phagocyte growth factor, CSF-1. Cell. 1985;41:665-676.
10. Bartelmez SH, Stanley ER. Synergism between hemopoietic growth factors (HGFs) detected by their effects on cells bearing receptors for a lineage specific HGF: assay of hemopoietin-1. J Cell Physiol. 1985;122:370-378.
11. Bartelmez SH, Sacca R, Stanley ER. Lineage specific receptors used to identify a growth factor for developmentally early hemopoietic cells: assay of hemopoietin 2. J Cell Physiol. 1985;122: 362-369.
12. Tushinski RJ, Oliver IT, Guilbert LJ, Tynan PW, Warner JR, Stanley ER. Survival of mononuclear phagocytes depends on a lineage-specific growth factor that the differentiated cells selectively destroy. Cell. 1982;28:71-81.
13. Stanley ER, Guilbert LJ, Tushinski RJ, Bartelmez SH. CSF-1—a mononuclear phagocyte lineage-specific hemopoietic growth factor. J Cell Biochem. 1983;21:151-159.
14. Suzumura A, Sawada M, Yamamoto H, Marunouchi T. Effects of colony stimulating factors on isolated microglia in vitro. J Neuroimmunol. 1990;30: 111-120.
15. Thery C, Mallat M. Influence of interleukin-1 and tumor necrosis factor alpha on the growth of microglial cells in primary cultures of mouse cerebral cortex: involvement of colony-stimulating factor 1. Neurosci Lett. 1993;150:195-199.
16. Hofstetter W, Wetterwald A, Cecchini MG, Fleisch H, Stanley ER, Felix R. Binding sites for macrophage colony-stimulating factor (M-CSF) are expressed on osteoclasts and their precursors (abstract 1063). J Bone Min Res. 1993;8(suppl 1): S382.
17. Baker AH, Ridge SA, Hoy T, et al. Expression of the colony-stimulating factor 1 receptor in B lymphocytes. Oncogene. 1993;8:371-378.
18. Till KJ, Lopez A, Slupsky J, Cawley JC. C-fms protein expression by B-cells, with particular reference to the hairy cells of hairy-cell leukemia. Br J Haematol. 1993;83:223-231.
19. Inaba T, Yamada N, Gotoda T, et al. Expression of M-CSF receptor encoded by c-*fms* on smooth muscle cells derived from arteriosclerotic lesion. J Biol Chem. 1992;267:5693-5699.
20. Wang Y, Berezovska O, Fedoroff S. Expression of colony stimulating factor-1 receptor (CSF-1R) by CNS neurons in mice. J Neurosci Res. 1999;57: 616-632.
21. Murase S, Hayashi Y. Expression pattern and neurotrophic role of the c-*fms* proto-oncogene M-CSF receptor in rodent Purkinje cells. J Neurosci. 1998;24:10481-10492.
22. Takashima A, Edelbaum D, Kitajima T, et al. Colony-stimulating factor-1 secreted by fibroblasts promotes the growth of dendritic cell lines (XS series) derived from murine epidermis. J Immunol. 1995;154:5128-5135.
23. Arceci RJ, Pampfer S, Pollard JW. Expression of CSF-1/c-*fms* and SF/c-*kit* mRNA during preimplantation mouse development. Dev Biol. 1992; 151:1-8.
24. Arceci RJ, Shanahan F, Stanley ER, Pollard JW. Temporal expression and location of colony-stimulating factor 1 (CSF-1) and its receptor in the female reproductive tract are consistent with CSF-1-regulated placental development. Proc Natl Acad Sci U S A. 1989;86:8818-8822.
25. Regenstreif LJ, Rossant J. Expression of the c-fms proto-oncogene and of the cytokine, CSF-1, during mouse embryogenesis. Dev Biol. 1989; 133:284-294.
26. Arceci RJ, Pampfer S, Pollard JW. Role and expression of colony stimulating factor-1 and steel factor receptors and their ligands during pregnancy in the mouse. Reprod Fertil Dev. 1992;4: 619-632.
27. Bartelmez SH, Bradley TR, Bertoncello I, et al. Interleukin 1 plus interleukin 3 plus colony-stimulating factor 1 are essential for clonal proliferation of primitive myeloid bone marrow cells. Exp Hematol. 1989;17:240-245.
28. Marks SC Jr, Lane PW. Osteopetrosis, a new recessive skeletal mutation on chromosome 12 of the mouse. J Hered. 1976;67:11-18.
29. Yoshida H, Hayashi S-I, Kunisada T, et al. The murine mutation “osteopetrosis” (op) is a mutation in the coding region of the macrophage colony stimulating factor (Csfm) gene. Nature. 1990;345:442-444.
30. Wiktor-Jedrzejczak W, Bartocci A, Ferrante AW Jr, et al. Total absence of colony-stimulating factor 1 in the macrophage-deficient osteopetrotic (*op/op*) mouse. Proc Natl Acad Sci U S A. 1990; 87:4828-4832.
31. Begg SK, Radley JM, Pollard JW, Chisholm OT, Stanley ER, Bertoncello I. Delayed hematopoietic development in osteopetrotic (*op/op*) mice. J Exp Med. 1993;177:237-242.
32. Begg SK, Bertoncello I. The hematopoietic deficiencies in osteopetrotic (*op/op*) mice are not permanent, but progressively correct with age. Exp Hematol. 1993;21:493-495.
33. Niida S, Kaku M, Amano H, et al. Vascular endothelial growth factor can substitute for macrophage colony-stimulating factor in the support of osteoclastic bone resorption. J Exp Med. 1999; 190:293-298.
34. Wiktor-Jedrzejczak W, Ahmed A, Szczylik C, Skelly RR. Hematological characterization of congenital osteopetrosis in *op/op* mouse. J Exp Med. 1982;156:1516-1527.
35. Felix R, Cecchini MG, Hofstetter W, Elford PR, Stutzer A, Fleisch H. Impairment of macrophage colony-stimulating factor production and lack of resident bone marrow macrophages in the osteopetrotic *op/op* mouse. J Bone Min Res. 1990;5: 781-789.
36. Borycki A-G, Lenormand J-L, Guillier M, Smadja F, Stanley ER, Leibovitch SA. Co-expression of CSF-1 and its receptor on myoblasts is lost on their differentiation to myotubes. Exp Cell Res. 1995;218:213-222.
37. Ryan GR, Dai X-M, Dominguez M, et al. Rescue of the colony stimulating factor 1 (CSF-1)-nullizygous mouse *Csf1*^{op}/*Csf1*^{op} phenotype with a CSF-1 transgene and identification of sites of local CSF-1 synthesis. Blood. 2001;98:78-84.
38. Stanley ER. Colony-stimulating factor (CSF) radioimmunoassay: detection of a CSF subclass stimulating macrophage production. Proc Natl Acad Sci U S A. 1979;76:2969-2973.
39. Stanley ER. The macrophage colony-stimulating factor, CSF-1. Methods Enzymol. 1985;116:564-587.
40. Sundquist KT, Cecchini MG, Marks SC Jr. Colony-stimulating factor-1 injections improve but do not cure skeletal sclerosis in osteopetrotic (op) mice. Bone. 1995;16:39-46.
41. Gouon-Evans V, Rothenberg ME, Pollard JW. Postnatal mammary gland development requires macrophages and eosinophils. Development. 2000;127:2269-2282.
42. Cohen PE, Chisholm O, Arceci RJ, Stanley ER, Pollard JW. Absence of colony-stimulating factor-1 in osteopetrotic (*csfm*^{op}/*csfm*^{op}) mice results in male fertility defects. Biol Reprod. 1996;55: 310-317.
43. O’Gorman M. Phenotypic analysis. In: Robinson J, Darzynkiewicz Z, Dean PN, et al, eds. Current

Protocols in Cytometry. New York, NY: John Wiley and Sons; 1997:6.0.1-6.7.10.

44. Stanley ER. Murine bone marrow-derived macrophages. In: Walker JM, Pollard JW, eds. Animal Cell Culture. 2nd ed. Clifton, NJ: Humana Press; 1997:301-304.
45. Laemmli UK. Cleavage of structural proteins during the assembly of the head of bacteriophage T4. Nature. 1970;227:680-685.
46. Wang Y, Yeung YG, Stanley ER. CSF-1 stimulated multiubiquitination of the CSF-1 receptor and of Cbl follows their tyrosine phosphorylation and association with other signaling proteins. J Cell Biochem. 1999;72:119-134.
47. Michaelson MD, Bieri PL, Mehler MF, et al. CSF-1 deficiency in mice results in abnormal brain development. Development. 1996;122:2661-2672.
48. Bartocci A, Mastrogiannis DS, Migliorati G, Stockert RJ, Wolkoff AW, Stanley ER. Macrophages specifically regulate the concentration of their own growth factor in the circulation. Proc Natl Acad Sci U S A. 1987;84:6179-6183.
49. Lieschke GJ, Stanley E, Grail D, et al. Mice lacking both macrophage- and granulocyte-macrophage colony-stimulating factor have macrophages and coexistent osteopetrosis and severe lung disease. Blood. 1994;84:27-35.
50. Naito M, Hayashi S, Yoshida H, Nishikawa S, Shultz LD, Takahashi K. Abnormal differentiation of tissue macrophage populations in "osteopetrosis" (op) mice defective in the production of macrophage colony-stimulating factor. Am J Pathol. 1991;139:657-667.
51. Pollard JW, Hunt JS, Wiktor-Jedrzejczak W, Stanley ER. A pregnancy defect in the osteopetrotic (op/op) mouse demonstrates the requirement for CSF-1 in female fertility. Dev Biol. 1991;148:273-283.
52. Pollard JW, Bartocci A, Arceci R, Orlofsky A, Ladner MB, Stanley ER. Apparent role of the macrophage growth factor, CSF-1, in placental development. Nature. 1987;330:484-486.
53. Cohen PE, Zhu L, Pollard JW. Absence of colony stimulating factor-1 in osteopetrotic (csfmop/csfmop) mice disrupts estrous cycles and ovulation. Biol Reprod. 1997;56:110-118.
54. Cohen PE, Hardy MP, Pollard JW. Colony-stimulating factor-1 plays a major role in the development of reproductive function in male mice. Mol Endocrinol. 1997;11:1636-1650.
55. Guleria I, Pollard JW. The trophoblast is a component of the innate immune system during pregnancy. Nat Med. 2000;6:589-593.
56. Pollard JW, Hennighausen L. Colony stimulating factor 1 is required for mammary gland development during pregnancy. Proc Natl Acad Sci U S A. 1994;91:9312-9316.
57. Roth P, Dominguez MG, Stanley ER. The effects of colony-stimulating factor-1 on the distribution of mononuclear phagocytes in the developing osteopetrotic mouse. Blood. 1998;91:3773-3783.
58. Rudolph AM. Hepatic and ductus venosus blood flows during fetal life. Hepatology. 1983;3:254-258.
59. Hume DA, Favot P. Is the osteopetrotic (op/op mutant) mouse completely deficient in expression of macrophage colony-stimulating factor? J Interferon Cytokine Res. 1995;15:279-284.
60. Myint YY, Miyakawa K, Naito M, et al. Granulocyte/macrophage colony-stimulating factor and interleukin-3 correct osteopetrosis in mice with osteopetrosis mutation. Am J Pathol. 1999;154:553-566.
61. Bradley TR, Metcalf D. The growth of mouse bone marrow cells in vitro. Aust J Exp Biol Med Sci. 1966;44:287-299.
62. Tagaya H, Kunisada T, Yamazaki H, et al. Intramedullary and extramedullary B lymphopoiesis in osteopetrotic mice. Blood. 2000;95:3363-3370.
63. Lu L, Osmond DG. Regulation of cell survival during B lymphopoiesis in mouse bone marrow: enhanced pre-B-cell apoptosis in CSF-1-deficient op/op mutant mice. Exp Hematol. 2001;29:596-601.
64. Roussel MF, Dull TJ, Rettenmier CW, Ralph P, Ullrich A, Sherr CJ. Transforming potential of the c-fms proto-oncogene (CSF-1 receptor). Nature. 1987;325:549-552.
65. Woolford J, McAuliffe A, Rohrschneider LR. Activation of the feline c-fms proto-oncogene: multiple alterations are required to generate a fully transformed phenotype. Cell. 1988;55:965-977.
66. Van der Geer P, Hunter T. Tyrosine 706 and 807 phosphorylation site mutants in the murine colony-stimulating factor-1 receptor are unaffected in their ability to bind or phosphorylate phosphatidylinositol-3 kinase but show differential defects in their ability to induce early response gene transcription. Mol Cell Biol. 1991;11:4698-4709.
67. Rohrschneider LR, Metcalf D. Induction of macrophage colony-stimulating factor-dependent growth and differentiation after introduction of the murine c-*fms* gene into FDC-P1 cells. Mol Cell Biol. 1989;9:5081-5092.
68. Kato J-Y, Roussel MF, Ashmun RA, Sherr CJ. Transduction of human colony-stimulating factor-1 (CSF-1) receptor into interleukin-3-dependent mouse myeloid cells induces both CSF-1-dependent and factor-independent growth. Mol Cell Biol. 1989;9:4069-4073.
69. Hamilton JA. CSF-1 signal transduction: what is of functional significance? Immunol Today. 1997;18:313-317.
70. Hamilton JA. CSF-1 signal transduction. J Leukoc Biol. 1997;62:145-155.
71. Price LKH, Choi HU, Rosenberg L, Stanley ER. The predominant form of secreted colony stimulating factor-1 is a proteoglycan. J Biol Chem. 1992;267:2190-2199.
72. Mochizuki DY, Eisenman JR, Conlon PJ, Larsen AD, Tushinski RJ. Interleukin 1 regulates hematopoietic activity, a role previously ascribed to hemopoietin 1. Proc Natl Acad Sci U S A. 1987;84:5267-5271.
73. Zhou YQ, Stanley ER, Clark SC, et al. Interleukin-3 and interleukin-1 alpha allow earlier bone marrow progenitors to respond to human colony-stimulating factor 1. Blood. 1988;72:1870-1874.
74. Nakano T, Kodama H, Honjo T. Generation of lymphohematopoietic cells from embryonic stem cells in culture. Science. 1994;265:1098-1101.
75. Pawlak G, Grasset M, Arnaud S, Blanchet J, Mouchiroud G. Receptor for macrophage colony-stimulating factor transduces a signal decreasing erythroid potential in the multipotent hematopoietic EML cell line. Exp Hematol. 2000;28:1164-1173.

2002 99: 111-120
doi:10.1182/blood.V99.1.111

Targeted disruption of the mouse colony-stimulating factor 1 receptor gene results in osteopetrosis, mononuclear phagocyte deficiency, increased primitive progenitor cell frequencies, and reproductive defects

Xu-Ming Dai, Gregory R. Ryan, Andrew J. Hapel, Melissa G. Dominguez, Robert G. Russell, Sara Kapp, Vonetta Sylvestre and E. Richard Stanley

Blood (print ISSN 0006-4971, online ISSN 1528-0020), is published weekly by the American Society of Hematology, 2021 L St, NW, Suite 900, Washington DC 20036.